

# REINFORCED CONCRETE FIBER BEAM ELEMENT WITH BOND-SLIP

By Giorgio Monti<sup>1</sup> and Enrico Spacone,<sup>2</sup> Associate Member, ASCE

**ABSTRACT:** This paper presents a new reinforced concrete beam finite element that explicitly accounts for the slip between the reinforcing bars and the surrounding concrete. The element formulation combines the fiber-section model with the finite-element model of a reinforcing bar with continuous slip. The section model retains the plane-section assumption, but the steel fiber strains are computed as the sum of two contributions, the rebar deformation and the anchorage slip. The model applies to any cross-sectional shape under biaxial bending and both monotonic and cyclic loads. The model theoretical framework is presented first. A sensitivity study on the monotonic and cyclic response of a reinforcing bar shows how the model traces the bar's reduced initial stiffness, bond degradation, and anchorage loss for insufficient anchorage length. Finally, comparison with an experimental test on a circular column shows that the prediction with the new model is in good agreement with the test, whereas the original fiber model with perfect bond overestimates the hysteretic energy dissipated during the loading cycles.

## INTRODUCTION

Bond plays a fundamental role in the response of reinforced concrete (RC) members by allowing the stress transfer from the steel bars to the surrounding concrete. Perfect bond is usually assumed in the analysis of RC structures. This implies full compatibility between concrete and reinforcement strains. This assumption is valid only in regions where negligible stress transfer occurs between the two components (Kausler and Mehlhorn 1987). This can only take place at early loading stages and at low strain levels. As the load is increased, cracking as well as breaking of bond unavoidably occurs, and a certain amount of bond-slip takes place in the beam, all of which will in turn affect the stress distributions in both steel and concrete. Near the cracks, high bond-slips develop, causing relative displacements between concrete and the reinforcement steel. Due to this bond-slip, different strains are observed in the steel rebars and in the surrounding concrete.

Bond-slip affects the overall response of RC structural members. In particular, two phenomena are worth discussing:

- An increase in stiffness in the regions between two adjacent cracks. This effect, sometimes called *tension-stiffening*, can be included by either considering the tensile resistance of the concrete or by increasing the tensile stiffness and strength of the steel rebars. Tension-stiffening mostly affects the member response under serviceability conditions, because the effect of bond is completely lost when member failure occurs.
- An increase of flexibility at the member ends, due to the pullout of the rebars at the interface either with beam-column joints or with the footings. Similar drops in stiffness may also be caused by insufficient lap splices.

These effects become particularly important and complex under seismic loading conditions, when bond gradually deteriorates due to large strains and damage caused by the load reversals.

After a few years of successful application of the fiber beam

element to the analysis of RC structures, the introduction of the mechanics of bond-slip of the reinforcing bars appears to be a necessary enhancement toward a realistic description of the cyclic and ultimate behavior of RC structures. Rubiano-Benavides (1998) proposed the use of rotational springs at the element ends to account for the added flexibility due to bond-slip. This approach is more suitable for lumped plasticity models and requires particular care in the selection of the rotational spring's mechanical properties. The framework of the proposed model is that of the fiber model, where the rebar response is modified to account for the effects of bond-slip.

The basic idea is to merge the formulation of the reinforcing bar with bond-slip proposed by Monti et al. (1997a,b) into the force-based fiber element proposed by Spacone et al. (1996a). The framework of the fiber-section state determination is retained, and a new approach is proposed to compute the rebar stress and stiffness that includes the effects of slip.

In the new model, the steel fiber accounts not only for the response of the rebar inside the beam, but also for its anchorage outside the element, in either a structural joint or a footing. The steel fiber strain is given by the sum of the effects of the rebar deformation and the anchorage slip. The response is still computed in terms of fiber stress and stiffness, which are needed for the fiber-section state determination.

An attractive feature of this formulation is the possibility of tracing the response of each bar within a section, which is particularly important when each rebar undergoes a different load history. Therefore, the model is suitable for sections of general shape, including circular ones, and for sections under biaxial loading.

The theoretical framework of the new model is presented first, followed by a series of parametric studies on the performance of the new model. Finally, the results from an experimental test are compared with the prediction obtained with the proposed model.

## FIBER BEAM ELEMENT AND BAR ELEMENT WITH BOND-SLIP

The proposed finite element (FE) is based on two well-established formulations that are numerically stable and robust even in cases of element softening, when the moment capacity of an RC column decreases, typically due to crushing of the concrete fibers. The first formulation is that of a fiber beam element for the seismic analysis of RC structures (Spacone et al. 1996a), and the second represents the FE solution of the problem of a steel bar embedded in concrete (Monti et al. 1997a,b). Both formulations are based on the force method of structural analysis. The models account for material nonlinearities in steel, concrete, and bond under monotonic and cyclic loading.

<sup>1</sup>Assoc. Prof., Dip. di Ingegneria Strutturale e Geotecnica, Università La Sapienza, Via Gramsci, 53, 00197 Rome, Italy. E-mail: monti@uniroma1.it

<sup>2</sup>Asst. Prof., Dept. of Civ., Envir., and Arch. Engrg., Univ. of Colorado, Boulder, CO 80309-0428. E-mail: spacone@colorado.edu

Note. Associate Editor: Walter H. Gerstle. Discussion open until November 1, 2000. To extend the closing date one month, a written request must be filed with the ASCE Manager of Journals. The manuscript for this paper was submitted for review and possible publication on July 15, 1999. This paper is part of the *Journal of Structural Engineering*, Vol. 126, No. 6, June, 2000. ©ASCE, ISSN 0733-9445/00/0006-0654-0661/\$8.00 + \$.50 per page. Paper No. 21420.

The *fiber beam element* is made up of a series of sections along the element length, whose number and locations depend on the integration scheme. Fig. 1 shows an RC element with five integration points. The Gauss-Lobatto integration scheme is used here, because the positions of the first and last integration points always coincide with the end sections. The section response is obtained by integration of the stresses and stiffness across the section. These integrals are numerically evaluated by subdividing the section into small areas, or fibers. The beam response is then obtained through weighted integration of the section responses. The nonlinear behavior of the element derives entirely from the nonlinear constitutive responses of the concrete and steel fibers.

The fiber-section concept is general and can be used in both displacement-based and force-based elements. The proposed model uses the force approach presented in Spacone et al. (1996a). The element is based on assuming force interpolation functions along the element. The element accuracy stems from the fact that the force interpolation functions derive from equilibrium and are therefore “exact” for the beam case. The element implementation in a general purpose FE code requires an element state determination that is more involved than for a displacement-based element. In the original formulation by Spacone et al. (1996a), element iterations are used to find the section deformations that correspond to the nodal displacements. More recently, Neuenhofer and Filippou (1997) have shown that a single iteration is sufficient at the element level, because structural equilibrium will eventually ensure convergence at both element and section levels. At convergence, element equilibrium is satisfied pointwise along the element, and element compatibility is satisfied in an integral sense.

One limitation of fiber-section models proposed to date is the assumption of perfect bond between steel and concrete, which leads to neglecting the relative slip between the steel fibers and the surrounding concrete. It is important to note that this assumption affects the section state determination only, whereas the element framework, based on equilibrium between external and internal forces, remains valid.

The *bar element with bond-slip* can be regarded as a structural system consisting of two parallel components: (1) A reinforcing bar; and (2) the interface between the rebar and the surrounding concrete. The global response of the rebar depends on the interaction between the stress fields of both components. The element proposed by Monti et al. (1997a) is

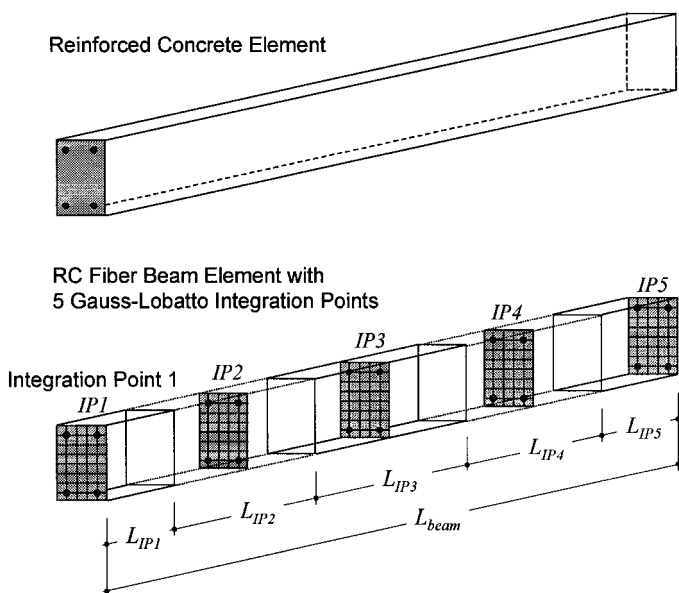


FIG. 1. Fiber Beam Element with Five Gauss-Lobatto Integration Points

based on a force approach in which the interpolation functions defining the stress field in the rebar satisfy equilibrium with bond stresses over the bar surface. The element allows solving the problem of a bar embedded in concrete. In particular, it can be used to find the stress and stiffness of a bar under prescribed displacements (pullout).

The major problem in implementing the bar model in a beam element derives from the fact that the rebar response is expressed in terms of stress-slip ( $\sigma-u$ ). To insert it into a fiber section, it is necessary to express the rebar response in terms of stress-strain ( $\sigma-\epsilon$ ), because the fiber-section state determination is performed based on an assigned strain distribution.

## RC FIBER BEAM ELEMENT WITH BOND-SLIP

The response of a beam element (mainly the element stiffness matrix and the element forces) is typically computed as a weighted sum of the responses of a discrete number of cross sections. The cross sections are located at control points whose locations depend on the numerical integration scheme. In force-based RC elements, a Gauss-Lobatto integration scheme often is preferred because its extreme integration points always coincide with the element end sections, where significant inelastic deformations typically take place.

The fiber beam element state determination is carried out at three levels—element, section, and fiber. At all three levels, the problem is the same: determine the forces (or stresses) and stiffness corresponding to prescribed deformations. In particular, the section state determination computes the section axial force and bending moment corresponding to prescribed section deformations, namely, the average axial strain  $\bar{\epsilon}$  and the section curvature  $\kappa$ . The discussion is limited here to the uniaxial bending case, but extension to the biaxial case is straightforward. From the plane-section assumption, the strain at a fiber located at a distance  $y$  from the reference axis is

$$\epsilon = \bar{\epsilon} + \kappa y \quad (1)$$

When perfect bond is assumed between concrete and steel rebar, concrete and steel fibers located at the same depth  $y$  have the same strain

$$\epsilon_s = \epsilon_c = \epsilon = \bar{\epsilon} + \kappa y \quad (2)$$

This assumption is removed to include the effects of bond-slip. The first step in this direction requires a more in-depth look at the beam element formulation.

Because of the numerical integration used to solve the element integrals, the beam element is modeled as a set of adjacent slices that are connected in series (Fig. 1). The element response is the weighted sum of the responses of each slice. If one considers a beam element of length  $L_{beam}$ , the length of each slice is  $L_{IP} = w_{IP} L_{beam}$ . The slice length  $L_{IP}$  is a function of the integration scheme, the number of integration points and thus the weight  $w_{IP}$  pertaining to the integration point  $IP$ .

Each slice can be considered as a parallel system made of two components, steel and concrete. From the assumption of perfect bond, the slice and its components have the same elongation  $\bar{d}$  and rotation  $\varphi$

$$\bar{d} = \bar{d}_c = \bar{d}_s; \quad \varphi = \varphi_c = \varphi_s \quad (3)$$

in which  $\bar{d}_c$ ,  $\bar{d}_s$  and  $\varphi_c$ ,  $\varphi_s$  = slice elongations and rotations in the concrete and steel components, respectively. The slice is basically a finite length of beam element  $L_{IP}$  with constant deformations. These are the axial strain  $\bar{\epsilon}$  and the curvature  $\kappa$  of the integration point  $IP$ , therefore

$$\bar{d} = \bar{\epsilon} L_{IP}; \quad \varphi = \kappa L_{IP} \quad (4)$$

With this notation, the compatibility condition of (2) can be expressed in terms of concrete and steel displacements. The elongation of a fiber at distance  $y$  from the reference axis can be written

$$u(y) = u_c = u_s = \bar{d} + \varphi y \quad (5)$$

From (1) and (4) the strain distribution  $\varepsilon(y)$  across the monitored section can be written

$$\varepsilon(y) = \frac{1}{L_{IP}} u(y) = \frac{1}{L_{IP}} (\bar{d} + \varphi y) \quad (6)$$

Based on these definitions, it is now possible to enhance the representation of the slice deformation by relaxing the assumption of perfect bond between steel and concrete. This can be done by assuming that the deformation of the steel component is due partly to the bar elongation and partly to the slip between the bar and the concrete. This is expressed in the following form:

$$\bar{d} = \bar{d}_c = \bar{d}_{s+a} = \bar{d}_s + \bar{d}_a; \quad \varphi = \varphi_c = \varphi_{s+a} = \varphi_s + \varphi_a \quad (7)$$

in which the slice axial deformation  $\bar{d}$  and the slice rotation  $\varphi$  are expressed as a sum of two contributions, one due to the rebar deformation (subscript  $s$ ), the other to the anchorage slip (subscript  $a$ ).

From (7), the concrete strain is the same as in (6)

$$\varepsilon(y_c) = \frac{1}{L_{IP}} (\bar{d}_c + \varphi_c y_c) = \bar{\varepsilon} + \kappa y_c \quad (8)$$

whereas the steel strain becomes

$$\varepsilon_{s+a} = \frac{1}{L_{IP}} (\bar{d}_s + \varphi_s y_s) + \frac{1}{L_{IP}} (\bar{d}_a + \varphi_a y_s) \quad (9)$$

in which the first term represents the strain of the steel bar in the slice and the second is the contribution of the bond-slip. Therefore

$$\varepsilon_{s+a} = \varepsilon_s + \frac{1}{L_{IP}} u_a = \varepsilon_s + \varepsilon_a \quad (10)$$

in which  $\varepsilon_a$  should be regarded as a strain-equivalent contribution of the anchorage pullout, condensed at the fiber level through the length  $L_{IP}$  of the integration point. In other words, the total steel fiber elongation is given by the sum of the rebar

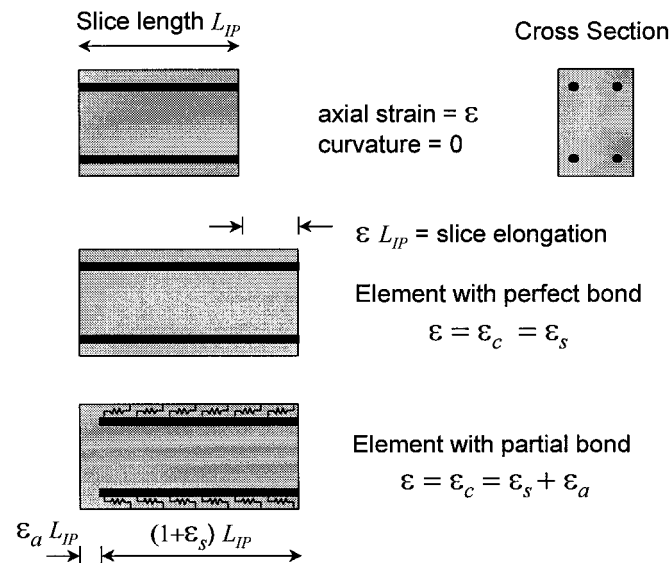


FIG. 2. Slice Response to Axial Deformation Only: Perfect Bond versus Partial Bond

deformation and anchorage pullout. Compatibility is maintained between the concrete strain and the total steel fiber elongation ( $\varepsilon_c = \varepsilon_{s+a}$ ), and concrete and steel strains are different ( $\varepsilon_c \neq \varepsilon_s$ ). This procedure is illustrated in Fig. 2 for the case of a slice with axial deformation only and no curvature.

It is important to point out that the proposed formulation provides a solution to the bond-slip problem within a single beam FE. The element can capture the base rotation in RC columns due to bar slips and can also describe slip and bond failure of the rebar splices. On the other hand, the bond-slip effects of bars that connect two beam elements through a beam-column joint cannot be captured by this formulation. The development of a beam-column joint element (currently missing) would be of significant help in modeling this type of interaction.

### Fiber-Section State Determination

The fiber-section state determination is identical to that presented in Spacone et al. (1996a). Given the section deformations  $\bar{\varepsilon}$  and  $\kappa$ , find the corresponding section forces and stiffness. The fiber strains  $\varepsilon(y) = \bar{\varepsilon} + \kappa y$  are computed first. Based on the new strain field, the fiber stresses and tangent moduli are computed. They are then integrated over the cross section to yield the section forces and stiffness. The main difference introduced by the new approach concerns the fiber response. Although the concrete strain is directly computed from (8), the steel strain determination is more involved because (9) yields the total steel response  $\varepsilon_{s+a}$ . A specific procedure has been developed to compute the rebar deformation  $\varepsilon_s$  and average anchorage slip  $\varepsilon_a$  corresponding to  $\varepsilon_{s+a}$ .

### Steel Fiber State Determination

The steel fiber state determination computes the rebar stress and stiffness corresponding to the total strain  $\varepsilon_{s+a} = \varepsilon_s + u_a/L_{IP}$ . The slip  $u_a$  is obtained by solving the FE problem of a bar along an embedment length  $L_a$ . This embedment length varies according to the position of the bar. For continuous bars along the beam length,  $L_a = L_{IP}$ . For spliced bars along the beam length,  $L_a$  equals the splice length. For bars anchored outside the beam element,  $L_a$  represents the slice length  $L_{IP}$  plus the anchorage length. This case is illustrated in Fig. 3, which shows the state determination of the top steel rebar at the beam's first integration point. The embedded bar is mod-

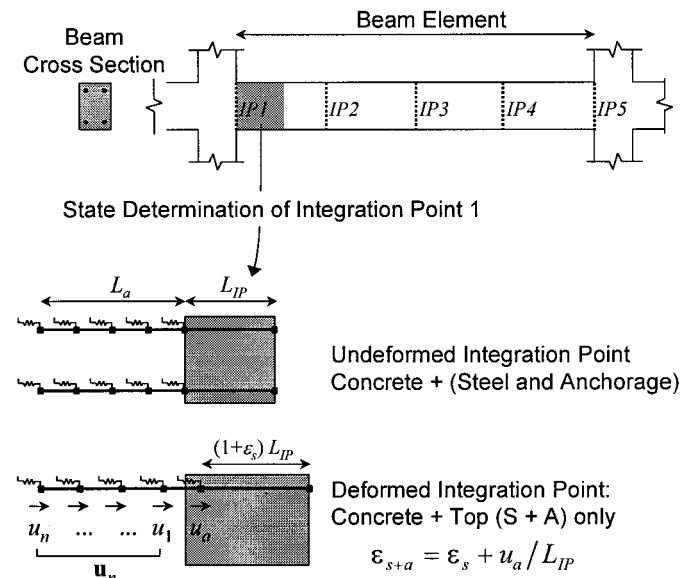


FIG. 3. Steel Bar State Determination Including Anchorage Slip

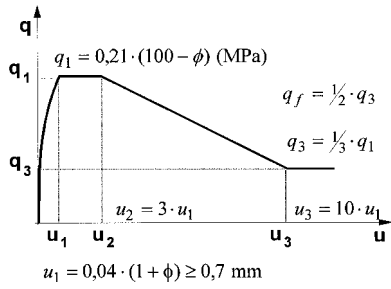


FIG. 4. Bond-Slip Constitutive Law (Eligehausen et al. 1983) with Parameters Based on Bar Diameter

eled by a series of  $n$  rebars embedded in concrete and under continuous bond, following the approach proposed by Monti et al. (1997a,b). The steel constitutive law is that of Menegotto and Pinto (1973), and the bond-slip constitutive law is that proposed by Eligehausen et al. (1983), shown in Fig. 4, where  $q_1$  is the bond-slip strength and  $q_f$  is the residual (frictional) bond strength. The steel response and the anchorage slip law are linearized as follows:

$$\sigma_s = E_s \varepsilon_s; \quad \begin{Bmatrix} \sigma_a \\ \mathbf{0} \end{Bmatrix} = \begin{bmatrix} k_{aa} & \mathbf{k}_{an} \\ \mathbf{k}_{na} & \mathbf{k}_{nn} \end{bmatrix} \begin{Bmatrix} u_a \\ \mathbf{u}_n \end{Bmatrix} \quad (11)$$

where the anchorage degrees of freedom (DOF) have been split into the anchorage displacement  $u_a$  and the displacements  $\mathbf{u}_n$  of the other  $n$  nodes along the anchorage length (Fig. 3). The  $\mathbf{0}$  vector in the stress vector indicates that the bar is subjected only to an end stress  $\sigma_a$ , whereas all other DOF have no applied stress. The last node  $n$  at the anchorage tip is therefore unrestrained. The value of  $n$  depends on the number of elements used to discretize the length  $L_a$  of the anchorage zone. A study on the optimal number of elements can be found in Monti et al. (1997a).

The length of the anchorage zone  $L_a$  is not necessarily equal to the length of the integration point  $L_{IP}$ . The value of  $L_a$  is the length of the bar from the section under consideration to its free end. Hence,  $L_a$  can represent either the anchorage length outside the beam (either in the footing or in another framing element) or the lap-splice length inside the element. No assumption is necessary on the effective anchorage length  $L_{a,eff}$  (i.e., the distance at which the relative slip drops to zero), because this is automatically computed in the solution of the embedded bar problem (Monti et al. 1997a). The same can be said for the rigid body motion of the entire anchorage due to complete slip-through, which occurs when  $L_a < L_{a,eff}$ . This phenomenon is described in the embedded bar formulation.

The following deformation vector  $\mathbf{e}$  is associated with each fiber

$$\mathbf{e} = \frac{1}{L_{IP}} \{L_{IP} \varepsilon_s \quad u_a \quad \mathbf{u}_n\}^T \quad (12)$$

Using this notation the strain in the “steel fiber + anchorage” system ( $s + a$ ) given by (10) is written

$$\varepsilon_{s+a} = \mathbf{m}^T \mathbf{e} \quad (13)$$

in which  $\mathbf{m} = \{1 \ 1 \ \mathbf{0}\}^T$ . A steel fiber stress vector  $\mathbf{s}$  is also defined

$$\mathbf{s} = \{\sigma_s \quad \sigma_a \quad \mathbf{s}_n^U\}^T \quad (14)$$

in which  $\mathbf{s}_n^U$  = stress unbalance vector at the nodes along the anchorage length. This unbalance is included because of the nonlinearity of the problem. During the solution process, it is likely to have  $\mathbf{s}_n^U \neq \mathbf{0}$ . When the anchorage solution is reached  $\mathbf{s}_n^U \rightarrow \mathbf{0}$ .

Due to the series arrangement of steel and anchorage ex-

pressed by (10), the steel fiber and the anchorage have the same applied stress

$$\sigma_{s+a} = \sigma_s = \sigma_a \quad (15)$$

which allows rewriting the stress vector of (14) as

$$\mathbf{s} = \mathbf{m} \sigma_{s+a} + \{0 \ 0 \ \mathbf{s}_n^U\}^T \quad (16)$$

The two local constitutive relationships (11) are grouped in a single expression

$$\mathbf{s} = \mathbf{K} \mathbf{e} = L_{IP} \begin{bmatrix} E_s/L_{IP} & 0 & \mathbf{0} \\ 0 & k_{aa} & \mathbf{k}_{an} \\ \mathbf{0} & \mathbf{k}_{na} & \mathbf{k}_{nn} \end{bmatrix} \mathbf{e} \quad (17)$$

### Steel Fiber Stiffness and Residual Strain Including Bond-Slip

The stiffness matrix in (17) can be built using the virtual force principle. The virtual force principle can then be written in the following form:

$$\delta \sigma_{s+a} \varepsilon_{s+a} = \delta \mathbf{s}^T \mathbf{e} \quad (18)$$

The virtual variation of the stress vector should be in equilibrium ( $\delta \mathbf{s}_n^U = \mathbf{0}$ ) and is given by

$$\delta \mathbf{s} = \mathbf{m} \delta \sigma_{s+a} \quad (19)$$

Upon substitution of (19) into (18) and after elimination of the virtual variation  $\delta \sigma_{s+a}$  from the standard argument of arbitrariness, (18) is written

$$\varepsilon_{s+a} = \mathbf{m}^T \mathbf{e} = \mathbf{m}^T \mathbf{K}^{-1} \mathbf{s} = \mathbf{m}^T \mathbf{F} \mathbf{s} \quad (20)$$

in which (17) has been substituted. The flexibility matrix  $\mathbf{F}$  is given by

$$\mathbf{F} = \mathbf{K}^{-1} = \frac{1}{L_{IP}} \begin{bmatrix} L_{IP}/E_s & 0 & \mathbf{0} \\ 0 & f_{aa} & \mathbf{f}_{an} \\ \mathbf{0} & \mathbf{f}_{na} & \mathbf{f}_{nn} \end{bmatrix} \quad (21)$$

Upon substitution of (16) into (20), one obtains

$$\varepsilon_{s+a} = \mathbf{m}^T \mathbf{F} \mathbf{m} \sigma_{s+a} + \mathbf{m}^T \mathbf{F} \begin{Bmatrix} 0 \\ 0 \\ \mathbf{s}_n^U \end{Bmatrix} \quad (22)$$

and (22) is inverted to yield

$$\sigma_{s+a} = E_{s+a} (\varepsilon_{s+a} - \varepsilon_n^U) \quad (23)$$

in which  $E_{s+a}$  = stiffness of the steel plus bond fiber

$$E_{s+a} = [\mathbf{m}^T \mathbf{F} \mathbf{m}]^{-1} = \left( E_s^{-1} + \frac{1}{L_{IP}} f_{aa} \right)^{-1} \quad (24)$$

and the strain

$$\varepsilon_n^U = \mathbf{m}^T \mathbf{F} \begin{Bmatrix} 0 \\ 0 \\ \mathbf{s}_n^U \end{Bmatrix} = \frac{1}{L_{IP}} \mathbf{f}_{an} \mathbf{s}_n^U \quad (25)$$

represents the residual strain due to the unbalanced forces along the anchorage length. As the solution approaches convergence,  $\varepsilon_n^U \rightarrow 0$ .

Eq. (23) expresses the global constitutive law of the steel fiber including the effect of bond-slip. The constitutive law contains the residual deformations at the nodes in which the anchorage is discretized. These residuals are explicitly included because they are not recovered when performing the anchorage state determination, but they are recovered during the external iterations on the steel-bond fiber (Neuenhofer and Filippou 1997). When global convergence is reached, these residuals converge to zero.

To define convergence for each steel-bond fiber, a residual deformation vector associated with the corresponding stress unbalance can be defined

$$\mathbf{e}^U = \frac{1}{L_{IP}} \{L_{IP} \boldsymbol{\varepsilon}_s^U \quad \mathbf{u}_a^U \quad \mathbf{u}_n^U\}^T \quad (26)$$

whose components yield, through (13), the residual strain of the steel-bond fiber

$$\boldsymbol{\varepsilon}_{s+a}^U = \mathbf{m}^T \mathbf{e}^U = \boldsymbol{\varepsilon}_s^U + \frac{\mathbf{u}_a^U}{L_{IP}} \quad (27)$$

Note that the residual strains  $\mathbf{u}_n^U$  along the anchorage are not included in this definition, because they are already included in the constitutive law.

The above procedure is used to compute the steel stress and stiffness corresponding to an applied strain history. The procedure has been implemented in a fiber-section model. Due to the nonlinear character of both the steel constitutive law and the anchorage behavior, an iterative procedure is needed. The force-based iteration scheme described in Spacone et al. (1996a) has been followed. The steps required for the implementation of the steel model in the fiber section are summarized in Appendix III.

### REINFORCING BAR STRESS-STRAIN RESPONSE INCLUDING BOND-SLIP

In this section the stress-strain response of a conventional steel rebar is compared with that of a rebar that includes the effect of bond-slip along its anchorage length. The responses are compared in terms of the stress-strain relationship. It should again be remarked that, for bars under bond-slip conditions, the stress-strain representation is an abstraction, used only to facilitate the implementation of the proposed formulation in the fiber-section framework. Therefore, the purpose of the comparison is purely speculative, although it clearly illustrates how bond-slip affects the bar response.

In the following, two numerical tests are presented: (1) A monotonic pullout test on a bar anchored on  $L_a = 20$  diameters; and (2) a cyclic pull-push test on a bar anchored on  $L_a = 40$  diameters. In the monotonic test, three degrees of bond are considered: (1) Full bond, which denotes a conventional steel fiber with no bond-slip; (2) normal bond; and (3) weak bond.

For the normal bond case, the bond law parameters are evaluated through the equations included in Fig. 4, whereas for the weak bond case the bond parameters defining the bond strength (i.e.,  $q$ ) have been reduced by 50%. These two latter tests represent two possible situations that can occur in practical cases. In the normal bond case the steel bar yields before bond reaches the plateau (represented by the bond stress  $q_1$  in Fig. 4), whereas weak bond refers to a case where bond breaks and softens before the steel bar reaches its yield strength. The normal bond case represents a bar with sufficient anchorage length to carry the applied end force, and the weak bond case represents a bar with insufficient anchorage.

From the monotonic responses shown in Fig. 5, a significant difference in the initial behavior of the bar can be observed. The initial stiffness in both the normal and weak bond cases is smaller than for the full bond case. This has notable consequences on those analyses aimed at predicting the initial stiffness of sections, members, and structures. When the effect of bond deformation is included (even if bond is strong as in the normal bond case), a certain stiffness reduction should be expected, which adds to that due to the initial cracking. This effect has been observed in numerical simulation of experimental tests where perfect bond is assumed (Spacone et al. 1996b). In this case, while the strength of the element/structure is, in general, predicted quite accurately, the initial stiffness is overestimated.

As for the anchored bar strength, the postyield phase of the normal bond case is practically identical to the full bond case. This is reasonable because, after the bar yields, the major contribution to the overall deformation is essentially localized at the bar pulled end. On the other hand, remarkable differences are noted on the entire response of the weak bond case. Here, the bond failure drastically changes the stress-strain behavior of the bar. While the bar remains elastic (and therefore practically rigid if compared to the slip deformations), the applied force is only equilibrated by the bond stresses along the bar surface. When bond progressively breaks along the anchorage length, the slippage penetrates the anchorage until it reaches the bar end. At this stage (corresponding to a 0.006 strain in Fig. 5), the bar starts slipping as a rigid body and the residual strength is that resisted only by friction along the bar surface.

For the cyclic loading study shown in Fig. 6, only the weak bond case is depicted for comparison with the full bond case. Similarly to the monotonic example, the normal bond case differs from the full bond case for the initial and unloading stiffness only. In the weak bond case, although the anchorage length is greater than for the monotonic case, the difference in the initial stiffness is still observed. This difference is also shown in the unloading branches after yielding of the rebar. The smaller stiffness of the bar with weak bond gives rise to smaller cycles and therefore to a lower dissipation capacity. The behavior changes abruptly when the anchored bar reaches the third cycle. The cyclic degradation of bond cumulated so far along the bar surface is such that the bar starts slipping as a whole. This transition is identified by a clear failure point followed by anchorage slip, which cannot be traced with a conventional model based on the full bond assumption.

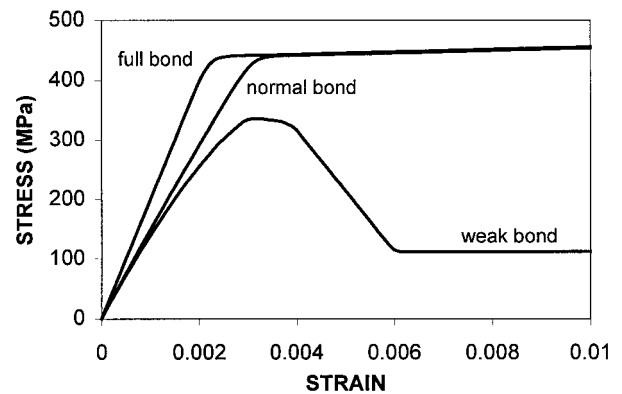


FIG. 5. Monotonic Stress-Strain Response of Reinforcing Bar Fiber with Different Degrees of Bond

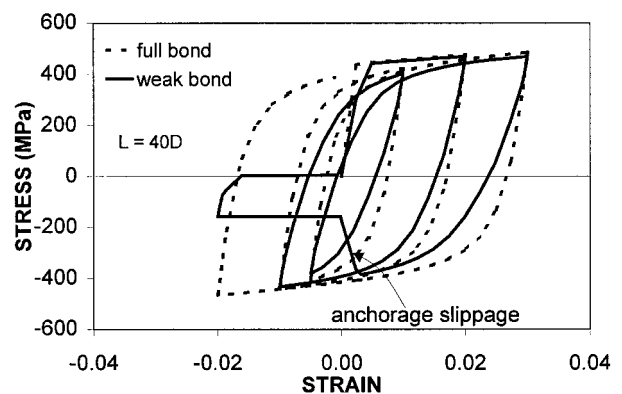


FIG. 6. Cyclic Stress-Strain Response of Reinforcing Bar with No Bond Slip and with Weak Bond

## COMPARISON WITH EXPERIMENTAL RESULTS

In this section a comparison with an experimental test by Saadatmanesh et al. (1996) is performed. The test was conducted on a scaled-down circular RC bridge column, designed according to obsolete seismic codes, with insufficient development lengths for the rebars anchored in the footing. Ready-mixed concrete with  $f'_c = 36.5$  MPa and steel with measured yield strength of 358 MPa were used. The height of the column was 2,000 mm, the diameter was 305 mm, and the longitudinal reinforcement was 14 bars of 13-mm diameter, resulting in a reinforcement ratio of 2.48%. Transverse confinement was provided by steel wire hoops of 3.5-mm diameter, spaced at 89 mm throughout the entire height of the column. The average yield stress for these wires was 301 MPa. In the specimen (denoted as C-1) the longitudinal reinforcement of the column was extended into the footing using starter bars that were lapped with the main longitudinal reinforcement of the column over a length of 20-bar diameters (254 mm). In the test an axial load of 445 kN was first applied to the column, followed by cyclic lateral displacements applied at the top of the column in both positive and negative directions according to the scheme:  $1u_y$ ,  $1.5u_y$ ,  $2u_y$ , and  $3u_y$ , where  $u_y$  is the yield displacement. At each displacement level, two cycles were performed. Fig. 7(a) shows the hysteresis loops for the experimental response of the circular column C-1 with lap splice (Saadatmanesh et al. 1996). The weak bond response already observed in the previous section characterizes the test. After the first cycle to  $u = 1.5u_y$ , there is a rapid degradation of the response due to progressive failure of the lapped reinforcement due to slip. In addition, it is noted that the cycles show significant pinching, with extremely reduced dissipation capacity. Fig. 7(b) presents two numerical simulations of the experimental test. The first was performed with the fiber-element model with perfect bond presented in Spacone et al. (1996a), the second uses the model proposed in this paper that includes bond-slip of the rebars. In both cases, for the FE model of the column, a single FE was used. This is one of the advantages of the force-based element with respect to a displacement-based element. The element precision leads to a significant saving in the number of elements. As for the step increment used in the numerical simulations, equal displacement increments of 1 mm were imposed at the column top. The overall test was simulated in a few minutes. The element precision leads to the use of very few structural DOF, which allows even large frames to be solved in a reasonable amount of time.

The differences in the prediction with the FE with no bond-slip are remarkable, the most evident regarding the dissipation capacity, which is of paramount importance in seismic analyses. When no bond-slip is considered, fuller cycles are predicted, which are far from being similar to those obtained in the test. On the other hand, the prediction obtained with the new model is similar to the experimental result. Another remarkable difference regards the prediction of the peak load cyclic degradation. The response obtained with the new model shows a decay that is very similar to the experimental case, thanks to its capacity of tracing the bond-damage penetration into the anchorage. As a matter of fact, a more sophisticated cyclic degradation rule in the bond-slip constitutive law would lead to further enhancements in the prediction capabilities of the proposed model, including a better estimate of the peak load and its degradation during the loading cycles. Finally, it is important to point out the complexity of the simulation in which the reinforcing bars all have different responses, because the steel is distributed along the perimeter of the circular RC section and all the rebars have different strains.

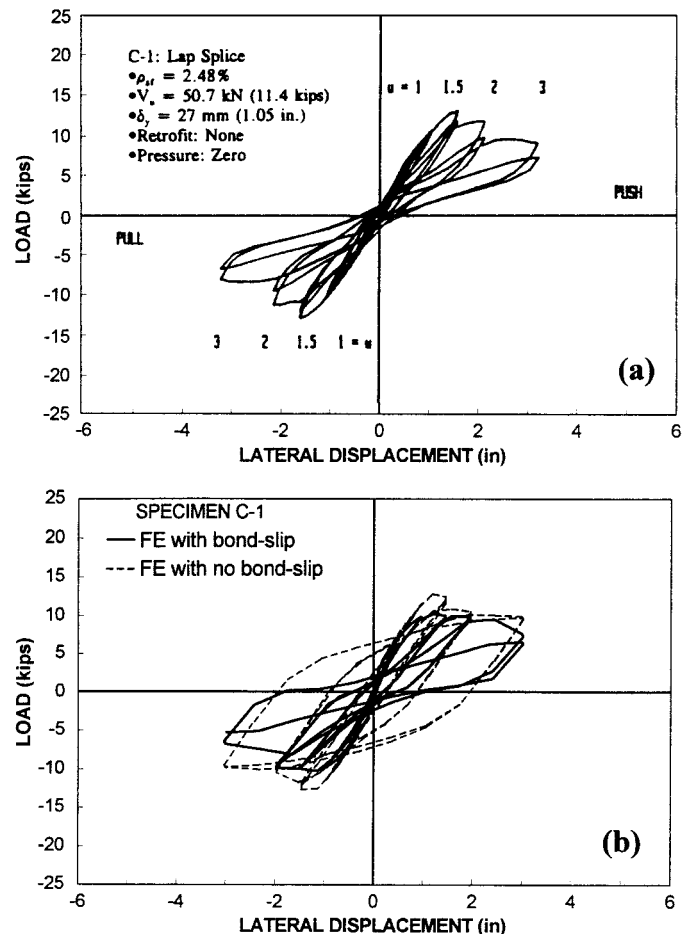


FIG. 7. Comparison between: (a) Experimental Test from Saadatmanesh et al. (1996); (b) Numerical Simulation with and without Bond-Slip

## SUMMARY AND CONCLUSIONS

A fiber beam element that includes bond-slip of the reinforcing bars has been presented. The formulation is derived from the force-based fiber beam element proposed by Spacone et al. (1996a), with the insertion of bar element with continuous bond developed by Monti et al. (1997a,b).

The response of the beam element is obtained through the weighted integration of the responses of the monitored sections along the element. The fiber-section response is computed by adding the contributions of all the concrete and steel fibers in which the section is subdivided. In the proposed beam element, the steel fiber state determination is modified to account for the bond-slip of the rebars. In the original model, the steel stress and stiffness are calculated directly from the steel constitutive law, based on the strain pertaining to the fiber. In the new model, the stress and stiffness of each steel fiber are obtained as the response of a bar that crosses the section under consideration and is anchored in the concrete. The end-slip can also be computed to give an estimate of the crack width. The implementation is simple and requires minor modifications to the structure of the original fiber beam element, provided a modular organization of the element routines is followed.

Because the new formulation affects the fiber-section model only and does not affect the overall element state determination, the proposed fiber-section model with bond-slip in the steel rebars can be implemented in any displacement-based or force-based element that uses a fiber-section discretization. In the present form the model is implemented in a force-based

element that is linked to the general purposed FE program FEAP (Taylor 1998).

Because each steel rebar in the cross section is monitored separately, the proposed model applies to cross sections of any shape. For the same reason, the model can be applied to both uniaxial and biaxial bending problems.

The new bar model has been used to show how the response of a reinforced bar embedded in concrete changes with different degrees of bond. Both monotonic and cyclic conditions have been considered. It was shown that the initial elastic stiffness of the steel rebar is reduced when the effect of bond is explicitly included. Although this consideration is not new, the proposed model computes the bar stiffness, including bond-slip, without the need of assuming an "effective anchorage length." This concept has no meaning if one thinks that the anchorage length of an embedded bar is not a fixed parameter but changes depending on the state of bond and the yield penetration along the bar. The possibility of predicting the initial stiffness has important implications in computing the initial stiffness and fundamental period of vibration of an RC frame. The model also allows, under large strains or repeated cyclic loads, to model bond deterioration and eventually the anchorage pullout.

Finally, a comparison between experimental data and numerical simulations has been presented. This study has shown that the results obtained with the proposed model correlate sufficiently well with the experimental data, particularly in the overall response shape, whereas the original fiber model with perfect bond largely overestimates the hysteretic energy dissipated during the loading cycles. Improvements to the cyclic degradation rules for the bond-slip law used in the study would further enhance the correlation with the experimental tests, especially in the prediction of the peak applied load.

The proposed model can be applied to the study of RC frames. For new structures it will provide a more realistic prediction of the initial stiffness than that obtained from the fiber model with perfect bond. For older structures with insufficient anchorage lengths or lap splices it can realistically account for bond degradation and pullout failure under both static and dynamic loading conditions.

## APPENDIX I. SUMMARY OF STEEL FIBER STATE DETERMINATION

The following steps summarize the procedure followed to implement the steel fiber with bond-slip in a fiber-section model:

1. Compute the strain increment  $\Delta \epsilon_{s+a}$  of the  $i$ th fiber

$$\Delta \epsilon_{s+a} = \Delta \bar{\epsilon} + \Delta \kappa \gamma \quad (28)$$

2. Determine the linearized stress increment and update the stress vector (in the first step  $\epsilon_n^U = 0$ )

$$\Delta \sigma_{s+a} = E_{s+a} (\Delta \epsilon_{s+a} - \epsilon_n^U) \quad (29)$$

$$\sigma_{s+a} = \sigma_{s+a} + \Delta \sigma_{s+a} \quad (30)$$

3. Compute the new stress increment vector

$$\Delta \mathbf{s} = \mathbf{m} \Delta \sigma_{s+a} \quad (31)$$

4. Find the strain increment vector  $\Delta \mathbf{e}$  and update the total deformations

$$\Delta \mathbf{e} = \{ \Delta \epsilon_s \quad \Delta u_a \quad \Delta \mathbf{u}_n \}^T = \mathbf{F} \Delta \mathbf{s} \quad (32)$$

$$\mathbf{e} = \mathbf{e} + \Delta \mathbf{e} \quad (33)$$

5. Perform the state determination for the steel and the anchorage

$$\epsilon_s \xrightarrow{SD} \sigma_s^R, \quad E_s \begin{Bmatrix} u_a \\ \mathbf{u}_n \end{Bmatrix} \xrightarrow{SD} \begin{Bmatrix} \sigma_a^R \\ \mathbf{s}_n^R \end{Bmatrix}; \quad \begin{bmatrix} k_{aa} & \mathbf{k}_{an} \\ \mathbf{k}_{na} & \mathbf{k}_{nn} \end{bmatrix} \quad (34)$$

6. Assemble the resisting stress vector and the local stiffness matrix. Compute the new global system stiffness  $E_{s+a}$

$$\mathbf{s}^R = \begin{Bmatrix} \sigma_s^R \\ \sigma_a^R \\ \mathbf{s}_n^R \end{Bmatrix}; \quad \mathbf{K} = L_{IP} \begin{bmatrix} E_s/L_{IP} & 0 & \mathbf{0} \\ 0 & k_{aa} & \mathbf{k}_{an} \\ \mathbf{0} & \mathbf{k}_{na} & \mathbf{k}_{nn} \end{bmatrix} \quad (35)$$

$$E_{s+a} = \left( E_s^{-1} + \frac{1}{L_{IP}} f_{aa} \right)^{-1} \quad (36)$$

7. Compute the stress unbalances

$$\mathbf{s}^U = \mathbf{s} - \mathbf{s}^R \quad (37)$$

8. Compute the residual strain vector

$$\mathbf{e}^U = \mathbf{K}^{-1} \mathbf{s}^U \quad (38)$$

9. Compute the strain residual in the steel + anchorage system and at the anchorage nodes

$$\epsilon_{s+a}^U = \mathbf{m}^T \mathbf{e}^U \quad (39)$$

$$\epsilon_n^U = \frac{1}{L_{IP}} \mathbf{f}_{an} \mathbf{s}_n^U \quad (40)$$

10. If the residual is smaller than a specified tolerance, then convergence has been reached, otherwise let  $\Delta \epsilon_{s+a} = -\epsilon_{s+a}^U$ , and go to Step 2.

## ACKNOWLEDGMENT

This work was partially sponsored by NATO Collaborative Research Grant No. 961189 and National Science Foundation Grant CMS-9804613. This support is gratefully acknowledged.

The opinions expressed in this paper are those of the writers only and do not reflect the views of the sponsoring agencies.

## APPENDIX II. REFERENCES

- Eligehausen, R., Popov, E. P., and Bertero, V. V. (1983). "Local bond stress-slip relationships of deformed bars under generalized excitations: Experimental results and analytical model." *EERC Rep. 83-23*, Earthquake Engrg. Res. Ctr., University of California, Berkeley, Richmond, Calif.
- Keuser, M., and Mehlhorn, G. (1987). "Finite element models for bond problems." *J. Struct. Engrg.*, ASCE, 113(10), 2160–2173.
- Menegotto, M., and Pinto, P. E. (1973). "Method of analysis for cyclically loaded reinforced concrete plane frames including changes in geometry and nonelastic behavior of elements under combined normal force and bending." *Proc., IABSE Symp. on Resistance and Ultimate Deformability of Struct. Acted on by Well-Defined Repeated Loads*, International Association for Bridge and Structural Engineering, Zurich, 112–123.
- Monti, G., Filippou, F. C., and Spacone, E. (1997a). "Finite element for anchored bars under cyclic load reversals." *J. Struct. Engrg.*, ASCE, 123(5), 614–623.
- Monti, G., Filippou, F. C., and Spacone, E. (1997b). "Analysis of hysteretic behavior of anchored reinforcing bars." *ACI Struct. J.*, 94(3), 248–261.
- Neuenhofer, A., and Filippou, F. C. (1997). "Evaluation of nonlinear frame finite-element models." *J. Struct. Engrg.*, ASCE, 123(7), 958–966.
- Rubiano-Benavides, N. R. (1998). "Predictions of the inelastic seismic response of concrete structures including shear deformations and anchorage slip." PhD dissertation, Dept. of Civ. Engrg., University of Texas, Austin, Tex.
- Saadatmanesh, H., Ehsani, M. R., and Jin, L. (1996). "Seismic strengthening of circular bridge pier models with fibre composites." *ACI Struct. J.*, 93(6), 639–647.
- Spacone, E., Filippou, F. C., and Taucer, F. F. (1996a). "Fibre beam-column model for nonlinear analysis of R/C frames. Part I: Formulation." *Earthquake Engrg. and Struct. Dyn.*, 25, 711–725.
- Spacone, E., Filippou, F. C., and Taucer, F. F. (1996b). "Fibre beam-

column model for nonlinear analysis of R/C frames. Part I: Applications." *Earthquake Engrg. and Struct. Dyn.*, 25, 727–742.  
 Taylor, R. L. (1998). *FEAP: A finite element analysis program. User's manual: Version 7.1*, Dept. of Civ. and Envir. Engrg., University of California, Berkeley, Calif.

### APPENDIX III. NOTATION

The following symbols are used in this paper:

$\bar{d}$  = slice elongation;  
 $\bar{d}_s, \bar{d}_c$  = elongation of steel and concrete slices, respectively;  
 $\bar{d}_{s+a}$  = slice elongation for steel fiber + anchorage system;  
 $E_s$  = steel fiber modulus;  
 $E_{s+a}$  = stiffness of steel fiber + anchorage system;  
 $\mathbf{e}$  = bar deformation vector;  
 $\mathbf{e}^U$  = residual deformation vector;  
 $\mathbf{F}$  = bar flexibility matrix;  
 $f_{aa}, \mathbf{f}_{an}, \mathbf{f}_{na}, \mathbf{f}_{nn}$  = terms in bar flexibility matrix;  
 $\mathbf{K}$  = bar stiffness matrix;  
 $k_{aa}, \mathbf{k}_{an}, \mathbf{k}_{na}, \mathbf{k}_{nn}$  = terms in bar stiffness matrix;  
 $L_a$  = bar anchorage length;  
 $L_{a,eff}$  = effective anchorage length;  
 $L_{IP}, L_{beam}$  = integration point length and beam length, respectively;  
 $\mathbf{m}$  = transformation vector between  $\mathbf{e}$  and  $\boldsymbol{\varepsilon}_{a+s}$ ;  
 $\mathbf{s}$  = bar stress vector;  
 $\mathbf{s}^R$  = bar resisting stress vector;  
 $\mathbf{s}_n^R$  = resisting stresses at  $n$  nodes along anchorage length;

$\mathbf{s}_n^U$  = stress unbalances at  $n$  nodes along anchorage length;  
 $u$  = fiber elongation;  
 $u_a$  = anchorage slip;  
 $u_s, u_c$  = elongation of steel and concrete fibers, respectively;  
 $\mathbf{u}_n$  = displacements at  $n$  nodes along anchorage length;  
 $u_y$  = yield displacement;  
 $w_{IP}$  = integration point weight;  
 $y$  = fiber distance from reference axis;  
 $\bar{\boldsymbol{\varepsilon}}$  = strain at reference axis;  
 $\boldsymbol{\varepsilon}$  = fiber strain;  
 $\boldsymbol{\varepsilon}_a$  = strain equivalent anchorage slip;  
 $\boldsymbol{\varepsilon}_s, \boldsymbol{\varepsilon}_c$  = steel and concrete fiber strains, respectively;  
 $\boldsymbol{\varepsilon}_{s+a}$  = strain for steel fiber + anchorage system;  
 $\boldsymbol{\varepsilon}_n^U$  = residual strain in steel-bond fiber;  
 $\boldsymbol{\kappa}$  = cross-section curvature;  
 $\sigma_a$  = stress at anchorage end;  
 $\sigma_s, \sigma_c$  = stresses in steel and concrete fibers, respectively;  
 $\sigma_s^R, \sigma_c^R$  = resisting stresses in steel and concrete fibers, respectively;  
 $\sigma_{s+a}$  = stress for steel fiber + anchorage system;  
 $\phi$  = steel bar diameter;  
 $\varphi$  = slice rotation;  
 $\varphi_s, \varphi_c$  = slice rotation for steel and concrete fibers, respectively; and  
 $\varphi_{s+a}$  = slice rotation for steel fiber + anchorage system.